N89-11085

MILLIMETER-WAVE STUDIES

Kenneth C. Allen
U.S. Department of Commerce
National Telecommunications and Information Administration
Institute for Telecommunication Sciences
325 Broadway
Boulder, CO 80303 USA

Abstract - Progress on millimeter-wave propagation experiments in Hawaii is reported. A short path for measuring attenuation in rain at 9.6, 28.8, 57.6, and 96.1 GHz is in operation. A slant path from Hilo to the top of Mauna Kea is scheduled. On this path, scattering from rain and clouds that may cause interference for satellites closely spaced in geosynchronous orbit will be measured at 28.8 and 96.1 GHz. In addition the full transmission matrix will be measured at the same frequencies on the slant path. The technique and equipment used to measure the transmission matrix are described.

1. Introduction

It is well-known that high rates of attenuation in rain will limit the availability of millimeter-wave telecommunication links. Fortunately, on Earth-satellite paths only a short segment of the path (depending on elevation angle and altitude of the ground station) is in the lower atmosphere where liquid water droplets occur. For this reason, millimeter waves may prove to be economically viable for a number of applications involving earth-space communications. To accurately predict the limitations that rain (and clouds) will place on such systems, a great deal more knowledge is needed about the interaction of millimeter waves and naturally occurring atmospheric hydrometeors.

A three-stage experiment measuring the effect of rain on some millimeter-wave propagation parameters is under way in Hawaii. The first stage of the experiment, to measure the dependence of the attenuation rate (dB/km) on rain rate (mm/h) at 9.6, 28.8, 57.6, and 96.1 GHz using a 1-km path on General Lyman Field in Hilo, Hawaii, is in progress. In the second stage, a slant path from the airfield to the top of Mauna Kea will be used to measure scattering from rain and clouds that may cause interference for satellites closely spaced in geosynchronous orbit. In the third stage, measurements of the complex transmission matrix at 28.8 and 96.1 GHz will be made on the same slant path.

The Hawaiian location was chosen because of the availability of a slant path from sea level to 4,205 m altitude, which would approximate the lower atmospheric portion of an earth-satellite path, on which rainfall is frequent (approximately 300 inches per year near mid-path).

The paths and equipment are described in the remainder of this report. The third stage (transmission matrix measurements) will be described before the second stage (interference measurements) to allow a more concise description of the equipment.

2. Short-Path Experiment

The purpose of the short path is to measure the attenuation rate (dB/km) in rain as a function of rain rate (mm/h) in the Hawaiian climate. Measurements have been made in the past in California, Colorado, and Alabama. This experiment extends the study of the climate dependence of attenuation in rain to Hawaii.

The short path has been in operation since February 23, 1988. The receivers at 9.6, 28.8, 57.6, and 96.1 GHz are located about 15 m above ground level in the old control tower on General Lyman Field in Hilo, Hawaii. The transmitters are located approximately 4 m above ground level on top of two standard scaffolding sections about 1 km south on the Shop and Yard grounds of the Hawaii Water Department. A tipping bucket and a laser rain rate gauge along with air and rain temperature measuring instruments are mounted on top of the old control tower. Hourly accumulated rainfalls measured with a tipping bucket are also available from the National Weather Service office located in the base of the tower. The radio frequency equipment has been described previously (Espeland et al., 1986).

The movement of most rain showers is north to south along the propagation path. The showers typically last for less than 30 minutes.

The data will be analyzed and reported in Fiscal Year 1989.

3. Transmission Matrix Measurements

Measurements of attenuation in rain are often made. However, rain has polarization dependent effects. More than attenuation measurements at a single polarization are needed to understand these effects. A more complete description of the propagation effects is provided by the transmission matrix.

3.1 Transmission Matrix

A transmitted, polarized wave can be represented by a complex valued, two element vector, E_t, the elements of which represent the phase and amplitude of two orthogonal polarization components of the wave, e.g., vertical and horizontal. When the wave is altered during propagation, a new vector, E_r, represents it at the receiver. The altered wave at the receiver can be related to the original using a 2x2, complex valued matrix, T, by

$$E_r = TE_t. \qquad (1)$$

The matrix T is called the transmission matrix and provides the desired description of the propagation characteristics of the path. See Figure 1.

3.2 Experiment

The planned experiment described here is to measure the transmission matrix at 28.8 and 96.1 GHz on a simulated earth-satellite path. This path from the old control tower on General Lyman Field, in Hilo, Hawaii to the top of Mauna Kea has an elevation angle of 5° and is 45.6 km long. The path profile is shown in Figure 2. When measuring the transmission matrix, it is

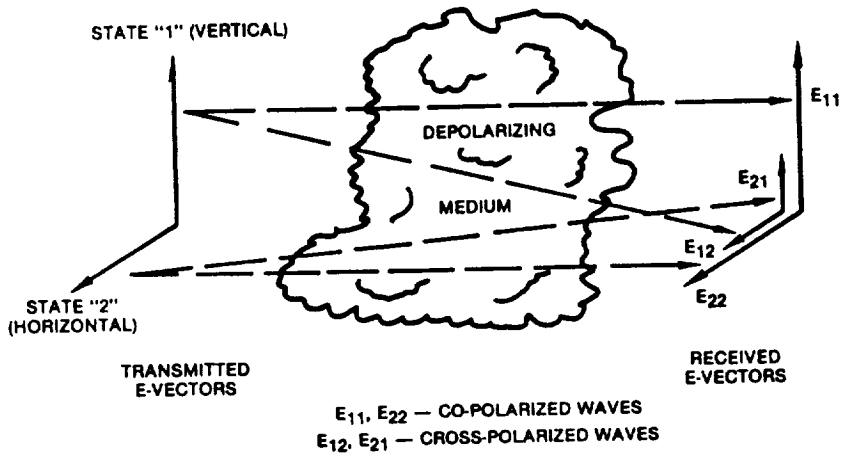

Figure 1. Depolarization (Ippolito et al., 1981).

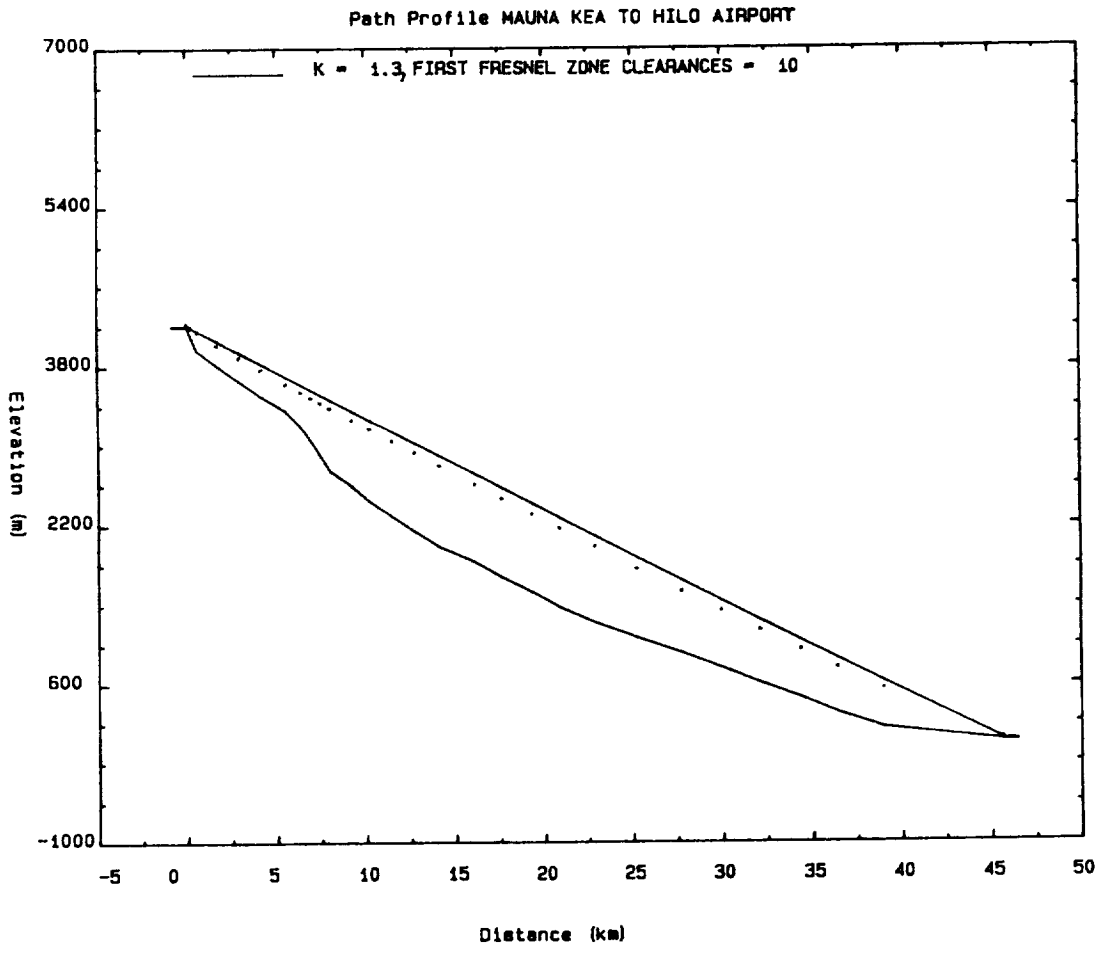

Figure 2. Path profile from the top of Mauna Kea to Hilo airport.

important to account for the effects of equipment that can be represented by additional matrices in (1). These effects will not be discussed here, but the reader can find a complete discussion in Marvira (1986).

The transmission matrix will be measured by transmitting vertically and horizontally polarized waves at slightly different frequencies. This allows the original polarization of the wave to be identified at the receiver. At the receiver, horizontal and vertical components will be received separately. There will be four IF's at the receiver corresponding to the waves transmitted vertically and received vertically, VV, transmitted vertically and received horizontally, VH, transmitted horizontally and received vertically, HV, and transmitted horizontally and received horizontally, HH. The phase and amplitude of these four IF's give the phase and amplitude of each of the elements in the transmission matrix.

Typically, transmission matrix measurements have been made by switching polarization devices at the transmitter and receiver. The technique described here has the advantages of allowing simultaneous measurements of phase at each polarization with a frequency response well in excess of 1 MHz μs.

3.3 Transmitters and Receivers

The phase of three of the transmission matrix elements can be measured with respect to the remaining one, usually one of the copolarization elements. However, the equipment for this experiment has been designed so that the phase delays of all four matrix elements at 28.8 and 96.1 GHz are measured with respect to the phase delay of the 9.6 GHz signal. This gives the additional information of the relative phase delays on the path of the different frequencies. The absolute phase delays could be measured, but variations in the absolute delay would make the measurements of the relative delays between the transmission matrix elements more difficult.

In Figure 3, a block diagram of the transmitters is presented. The 9.6-GHz signal serves as a phase reference for the receiver local oscillator. The 28.8 (vertical), 28.815 GHz (horizontal), 96.1 (vertical), and 96.15 GHz (horizontal) transmitted signals are all phase coherent with the 9.6 GHz signal, being derived from the same transmitter local oscillator (LO).

In Figure 4, a block diagram of the 9.6-GHz receiver and the reconstruction of the transmitter LO are shown. The 9.6-GHz received signal has a phase of

$$\phi_s = 1920\phi_{TLO} + 9.6\tau \qquad (2)$$

in wavelengths at 9.6 GHz where $20\phi_{TLO}$ is the phase of the 100-MHz transmitter LO and τ is the propagation delay of the 9.6-GHz wave in nanoseconds. All constant phase delays are neglected in this analysis.

The reference oscillator is phase locked to the received signal through Phase Lock Loop 1. The phase locking electronics (PLE) control the reference oscillator so that its phase and the phase of the IF output of the mixer are the same. This results in the reference oscillator frequency of

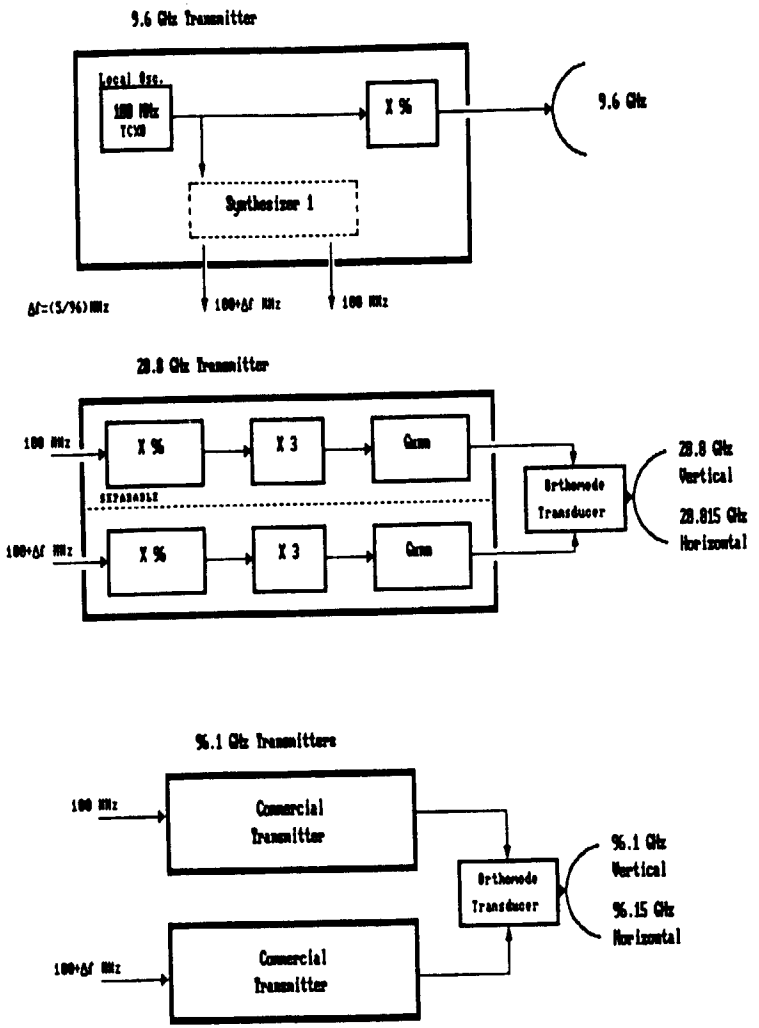

Figure 3. Block diagram of transmitters.

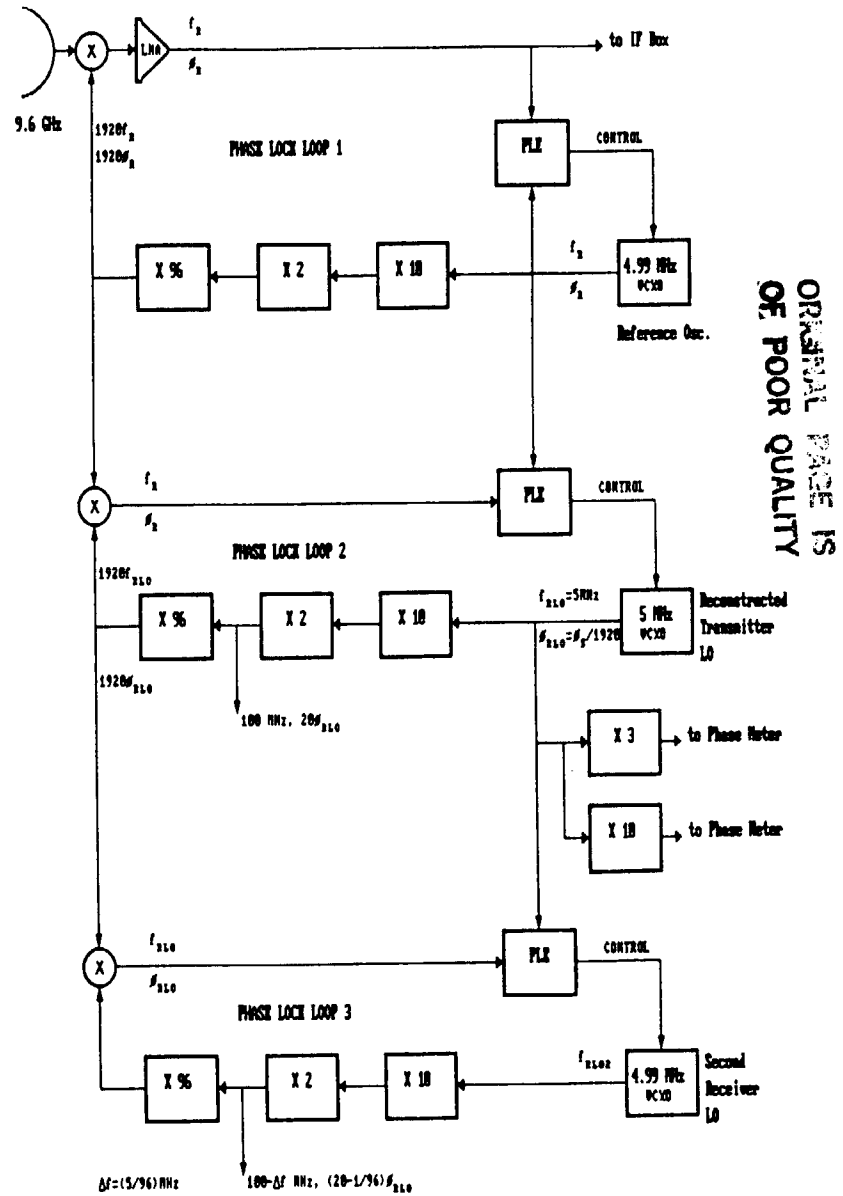

Figure 4. Block diagram of 9.6 GHz receiver and reconstruction of transmitter LO.

$$f_R = 9.6\ \text{GHz}/1921 = 5\ \text{MHz} \cdot 1920/1921 \tag{3}$$

and the phase of

$$\emptyset_R = \emptyset_S/1921. \tag{4}$$

In Phase Lock Loop 2 the reference oscillator signal is removed and the transmitter LO is reconstructed. In this second loop, the PLE controls the receiver LO so that the IF output of the mixer has the same phase as the reference oscillator. This results in the receiver LO frequency of

$$f_{RLO} = f_R \cdot 1921/1920 = 9.6\ \text{GHz}/1920 = 5\ \text{MHz} \tag{5}$$

and phase of

$$\emptyset_{RLO} = \emptyset_R\ 1921/1920 = \emptyset/1920 = \emptyset_{TLO} + 9.6\tau/1920. \tag{6}$$

Thus, the 5 MHz receiver LO is phase coherent with the phase of the 100 MHz transmitter LO plus the 9.6 GHz propagation delay phase divided by 1920. The 100 MHz signal with phase

$$20\emptyset_{RLO} = 20\emptyset_{TLO} + 9.6\tau/96 \tag{7}$$

is used in the 96-GHz receivers.

The purpose of Phase Lock Loop 3 is to generate a phase coherent LO signal at 100-Δf MHz for the other receivers. The PLE controls the second receiver LO so that the IF output of the mixer is the same as the receiver LO. Thus, the oscillator frequency is

$$f_{RLO2} = f_{RLO} \cdot 1919/1920 \tag{8}$$

so that when multiplied by 1920, it is 9.595 GHz or 5 MHz below the 9.6-GHz signal. In a similar fashion it results in proportional IF frequencies when used as the LO for 28.8 GHz of 15 MHz and for 96.1 GHz of 50 MHz. The (100-Δf)-MHz signal has a phase of $(20 - 1/96)\emptyset_{RLO}$.

In Figure 5, a conceptual block diagram of the receivers is presented. Each IF is sent to an IF processing box. There the IF's are amplified and filtered and fed into logarithmic amplifiers. The log amplifiers have limited outputs of the IF signal and analog outputs proportional to the logarithm of the IF amplitude. The analog outputs of signal amplitude are sent to an analog-to-digital (A/D) converter and recorded in a computer. The limited outputs are sent to phase meters. The analog outputs of the phase meters are sent to the A/D converter to be recorded in the computer.

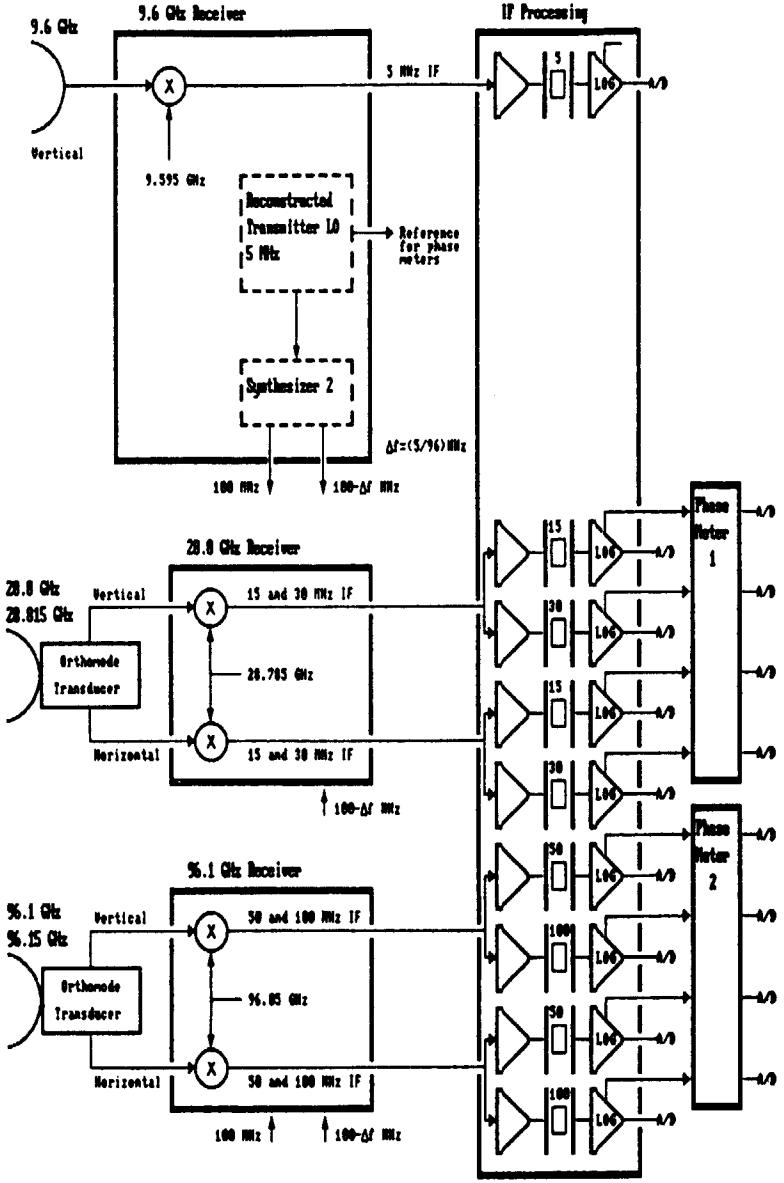

Figure 5. Block diagram of receivers.

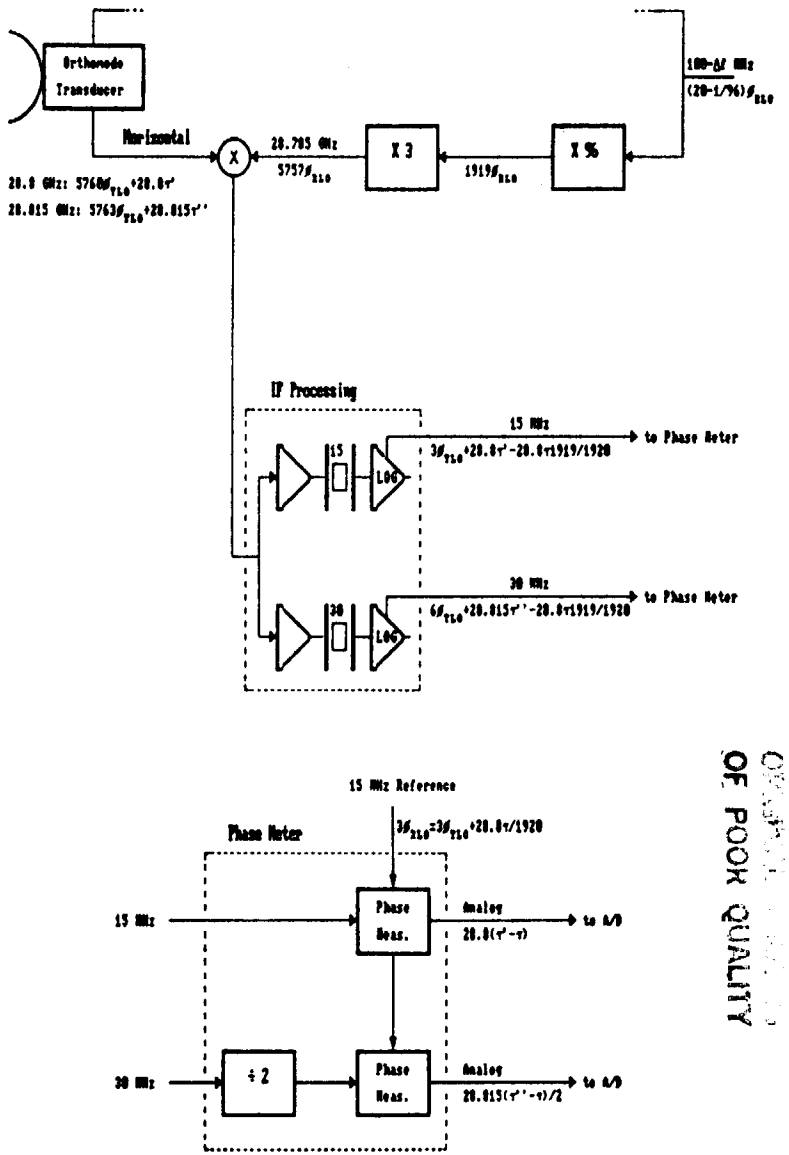

Figure 6. Example of phase analysis of 28.8 GHz receiver.

In Figure 6 an example of phase analysis is shown for the 28.8 GHz receiver. The phase of the 28.8-GHz VH signal (transmitted with vertical polarization and received with horizontal polarization) is 5760 $\emptyset_{TLO}$ + 28.8τ' where τ' is the delay time of this signal in nanoseconds. The phase of the 28.815-GHz HH signal is 5760 $\emptyset_{TLO}$ + 28.815τ'' where τ'' is the delay time of this signal. These two signals are mixed with the 28.785-GHz LO signal with phase 5757 $\emptyset_{RLO}$. The resultant IF's and their phases are shown in the figure. The output of the phase meter for the 15 MHz-VH IF is the propagation delay time at 28.8-GHz VH minus the propagation delay time at 9.6 GHz in 28.8-GHz wavelengths. The output for the 30 MHz HH IF is the propagation delay time at 28.815-GHz HH minus the delay time at 9.6 GHz in 28.815-GHz wavelengths. The results for the VV and HV signals follow similarly.

3.4. Phase Locking Electronics

The phase locking electronics (PLE) used in the transmitter and receiver are of a uniform design shown in Figure 7. Each signal is amplified to TTL levels and a digital phase comparison is done. The phase detector used is also a frequency detector so that even if the signals differ in frequency the control voltage will tune the VCXO until the frequencies are equal and then will lock the phase. Thus, phase lock is always achieved avoiding the problem with many phase lock loops in achieving or re-achieving lock. The frequency response of the phase detector and loop filter allow the tracking of phase shifts as rapid as 25 kHz.

3.5 Phase Meters

The phase meters were also designed to have fast response times. A block diagram of the phase meters is shown in Figure 8. The input signals can be as high as 100 MHz. Each input is amplified to ECL levels. These digital signals are then fed through a binary frequency divider capable of dividing by from 1 to 256. The dividing factor determines the scale of the analog output so that rapid folding over can be avoided. It also allows some flexibility in matching input and reference frequencies.

The phase measuring electronics can respond to phase shifts as rapid as one-half the frequency fed to it. The accuracy is about 2 to 3 degrees of the phase of the input to the measuring circuit so that the overall accuracy is scaled up by the dividing factor. The output is filtered before being fed to the A/D converter. Cutoff frequencies for these low-pass filters of 5 kHz are to be used initially.

4. Interference Measurements

The purpose of the interference measurements is to determine the potential of scattering from rain and clouds to cause interference on earth-satellite paths. One possible interference scenario is presented in Figure 9. Ground station B causes interference to satellite A receiving ground station A because energy from ground station B's beam directed at satellite B is scattered from the cloud toward satellite A. The geometry is the same for satellite A to interfere with ground station B receiving satellite B.

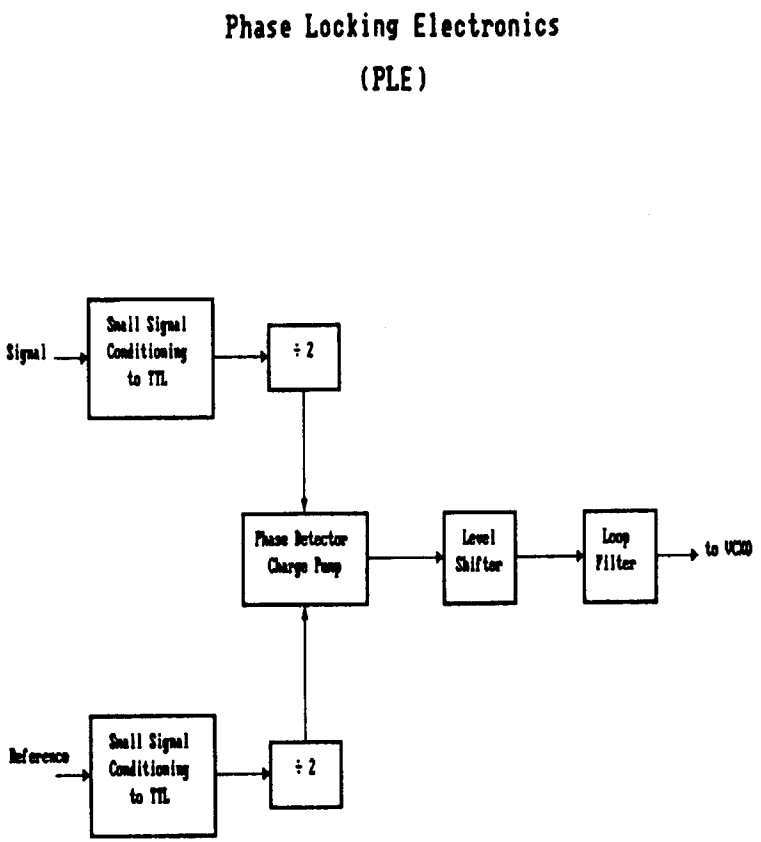

Figure 7. Block diagram of phase locking electronics.

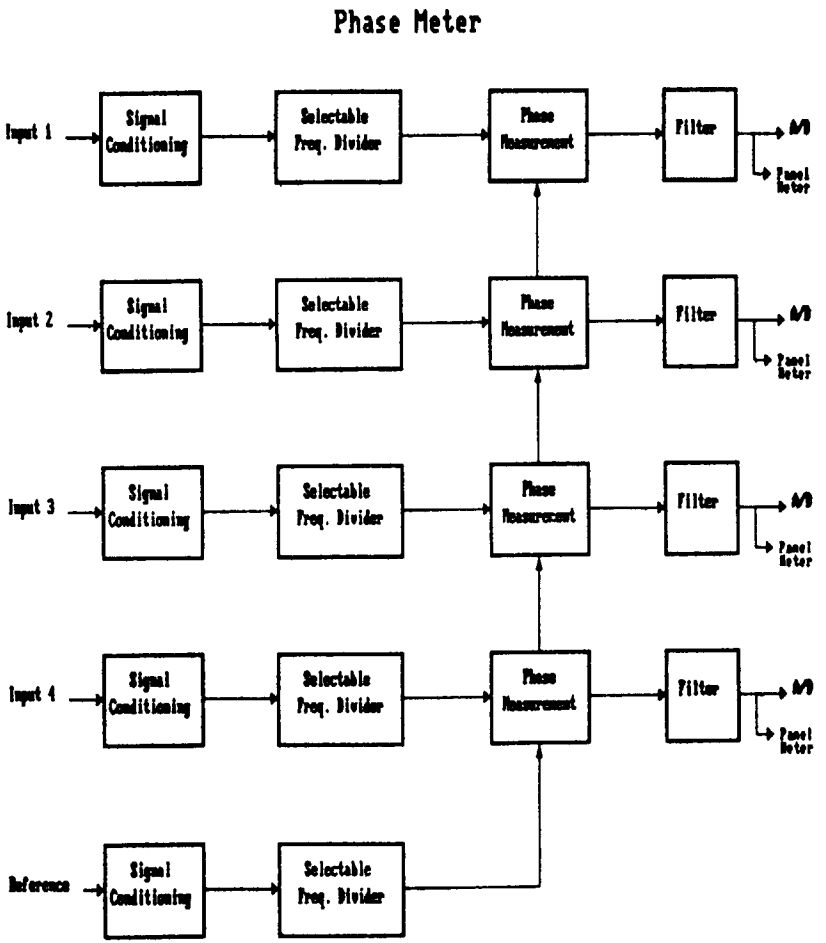

Figure 8. Block diagram of phase meters.

Figure 9. Geometry of earth-satellite path interference by scattering from rain and cloud.

Figure 10. Geometry of slant path interference measurements.

This interference scenario will be simulated as shown in Figure 10 employing the same equipment used for the transmission matrix measurements. The receivers at 9.6, 28.8, 28.815, 96.1, and 96.15 GHz will be located on top of Mauna Kea. The transmitters at 9.6, 28.815 and 96.15 GHz will be located in the old control tower but the transmitters at 28.8 and 96.1 GHz will be located on the scaffolding 1 km south of the old control tower. This will result in a separation of 1.2° degrees between the two transmitters as seen from the mountain top receivers. The receiving antennas will be pointed at the 28.8 and 96.1-GHz transmitters. Because of the narrow beamwidths and the shortness of the path, the other transmitters and the clouds above them are outside the receiving antenna beam. Therefore, the 28.815- and 96.15-GHz transmitting antennas will need to be pointed toward the clouds lying in the desired link. The scattering angles are still nearly forward as in the interference scenario being simulated.

The isolation between the desired transmitters and the interfering transmitters should be high (> 60 dB). Both signal levels will be monitored to measure how much this isolation is degraded by scattering from rain and clouds.

5. Summary

A description of a three-stage experiment has been presented. The first stage, measuring the specific attenuation in rain at 9.6, 28.8, 57.6, and 96.1 GHz in a tropical marine environment, is in progress in Hilo, Hawaii. The second stage will measure scattering from rain and clouds on a slant path from Hilo to the top of Mauna Kea. The third stage will measure the transmission matrix at 28.8 and 96.1 GHz on the same slant path.

The results of the experiments should be reported next fiscal year.

References

Espeland, R. H., E. J. Violette and K. C. Allen, "Rain attenuation measurements at 28.8, 57.6, and 96.1 GHz on a 1-km path," NTIA Report 86-190, 1986.

Ippolito, L. J., R. D. Kaul, and R. G. Wallace, "Propagation Effects Handbook for Satellite Systems Design," second ed., NASA Reference Publication 1082, December 1981.

Marvira, A., ed., Olympus Propagation Experiment Handbook for Data Preprocessing, Part 1: Theory and Basic Information, Issue 1, European Space Research and Technology Center, Noorduyk, The Netherlands, OPEX-11, Sept. 1986.